

# Competition and phylogeny determine community structure in Müllerian co-mimics

Markos A. Alexandrou<sup>1</sup>, Claudio Oliveira<sup>2</sup>, Marjorie Maillard<sup>1</sup>, Rona A. R. McGill<sup>3</sup>, Jason Newton<sup>3</sup>, Simon Creer<sup>1</sup> & Martin I. Taylor<sup>1</sup>

Until recently, the study of negative and antagonistic interactions (for example, competition and predation) has dominated our understanding of community structure, maintenance and assembly<sup>1</sup>. Nevertheless, a recent theoretical model suggests that positive interactions (for example, mutualisms) may counterbalance competition, facilitating long-term coexistence even among ecologically undifferentiated species<sup>2</sup>. Müllerian mimics are mutualists that share the costs of predator education<sup>3</sup> and are therefore ideally suited for the investigation of positive and negative interactions in community dynamics. The sole empirical test of this model in a Müllerian mimetic community supports the prediction that positive interactions outweigh the negative effects of spatial overlap<sup>4</sup> (without quantifying resource acquisition). Understanding the role of trophic niche partitioning in facilitating the evolution and stability of Müllerian mimetic communities is now of critical importance, but has yet to be formally investigated. Here we show that resource partitioning and phylogeny determine community structure and outweigh the positive effects of Müllerian mimicry in a species-rich group of neotropical catfishes. From multiple, independent reproductively isolated allopatric communities displaying convergently evolved colour patterns, 92% consist of species that do not compete for resources. Significant differences in phylogenetically conserved traits (snout morphology and body size) were consistently linked to trait-specific resource acquisition. Thus, we report the first evidence, to our knowledge, that competition for trophic resources and phylogeny are pivotal factors in the stable evolution of Müllerian mimicry rings. More generally, our work demonstrates that competition for resources is likely to have a dominant role in the structuring of communities that are simultaneously subject to the effects of both positive and negative interactions.

Positive interactions, such as mutualistic associations, can have important roles in the maintenance of community structure, potentially outweighing the negative effects of competition for niche space<sup>2</sup>. The empirical evidence for such phenomena is biased towards plants<sup>5,6</sup>, with a single study on mimetic butterfly communities<sup>4</sup> complementing such research. The study convincingly demonstrated that Müllerian mimic butterflies converge spatially, but it only considered habitat utilization, whereas resource consumption and trophic niche were indirectly inferred as likely correlates of other variables (such as forest structure, topography and flight height). However, until now the extent of trophic overlap or the evolution of morphological traits associated with resource acquisition has not been directly quantified in Müllerian mimetic communities and this limits our ability to infer the importance of mimicry in determining community structure. Combining ecological, phylogenetic and morphological analyses provides a valuable empirical test of the recent theoretical proposition<sup>2</sup> that positive interactions among competitors can promote multispecies coexistence and the consequences of these interactions in terms of species diversity<sup>7</sup>. Tropical freshwater fish offer a novel vertebrate perspective on the evolution of mimetic community structure, as they

inhabit discontinuous habitats and are exposed to a multitude of piscivorous predators<sup>8</sup>.

The Corydoradinae (Teleostei; Siluriformes; Callichthyidae) are a species-rich group of freshwater catfishes that inhabit streams, rivers and floodplains throughout South America<sup>9</sup>. The genus *Corydoras* comprises the majority of the Corydoradinae, and is the most species-rich genus of catfish with over 150 described species and as many undescribed taxa<sup>9,10</sup>. The Corydoradinae are almost all benthic omnivorous detritivores, consuming algae, terrestrial and aquatic insects, annelids and zooplankton<sup>11</sup>. At many sites, as many as three almost identically coloured species coexist and aggregate in large mixed shoals<sup>9,11,12</sup>, with each geographical location hosting a different shared colour pattern. These colour patterns include both cryptic and disruptive elements (for example, spots, counter-shading and eye bars) and putatively aposematic elements (for example, strongly contrasting black and white stripes, orange and black patches and conspicuously coloured spines). Interestingly, some colour patterns have also been adopted by species belonging to different families and orders (*Otocinclus*<sup>13</sup>, *Brachyrhamdia* and *Serrapinnus*).

In most cases, coexisting Corydoradinae species differ in snout morphology and body size<sup>11</sup>. Recorded predators of the Corydoradinae include *Plagioscion squamosissimus* (Perciformes)<sup>14</sup> and *Hoplias malabaricus* (Characiformes)<sup>11</sup>, whereas kingfishers, egrets and herons are the dominant avian predators of armoured catfishes<sup>15</sup>. Corydoradinae are protected by sharp, lockable pectoral and dorsal spines, tough scutes covering the side and dorsal surfaces<sup>10</sup>, and toxins secreted from the axillary glands<sup>16–18</sup>. The widespread distribution of Corydoradinae, propensity to aggregate, shared colour patterns and post-capture defences make them a unique system to study the mechanisms underpinning community structure.

A taxonomically comprehensive (80% coverage) phylogeny was constructed from 425 taxa (Supplementary Table 1) using Bayesian and maximum likelihood methods to resolve the relationships within the Corydoradinae and determine whether colour patterns are the result of convergence or shared ancestry (Fig. 1). Differences in tree topologies were small between mitochondrial and nuclear data sets, and both identified nine major lineages (Supplementary Figs 1–4). Using the resulting phylogeny, we identified 52 species belonging to 24 different mimicry rings, composed of two or three species each (Fig. 2). All lineages included taxa that were members of mimicry rings with the exception of lineage 2. A comparison of topological positions of respective co-mimics shows that 92% of mimetic communities are composed of species belonging to evolutionarily distinct lineages. In the only two mimetic groups with species belonging to the same genetic lineage, these are not sister species and apparent convergence may be due to close genetic affinity rather than convergence. As all other shared patterns are the product of convergence in sympatry, and all Corydoradinae are well protected, we consider Müllerian mimicry<sup>19</sup> to be the most convincing explanation for the pattern convergence. Patterns signalling unprofitability to predators do not have to be

<sup>1</sup>Environment Centre Wales, Molecular Ecology and Fisheries Genetics Laboratory, School of Biological Sciences, College of Natural Sciences, Bangor University, Bangor LL57 2UW, UK. <sup>2</sup>Departamento de Morfologia, Instituto de Biociências, Universidade Estadual Paulista, 18618-970 Botucatu, SP, Brazil. <sup>3</sup>NERC Life Sciences Mass Spectrometry Facility, Scottish Universities Environmental Research Centre, Rankine Avenue, East Kilbride G75 0QF, UK.

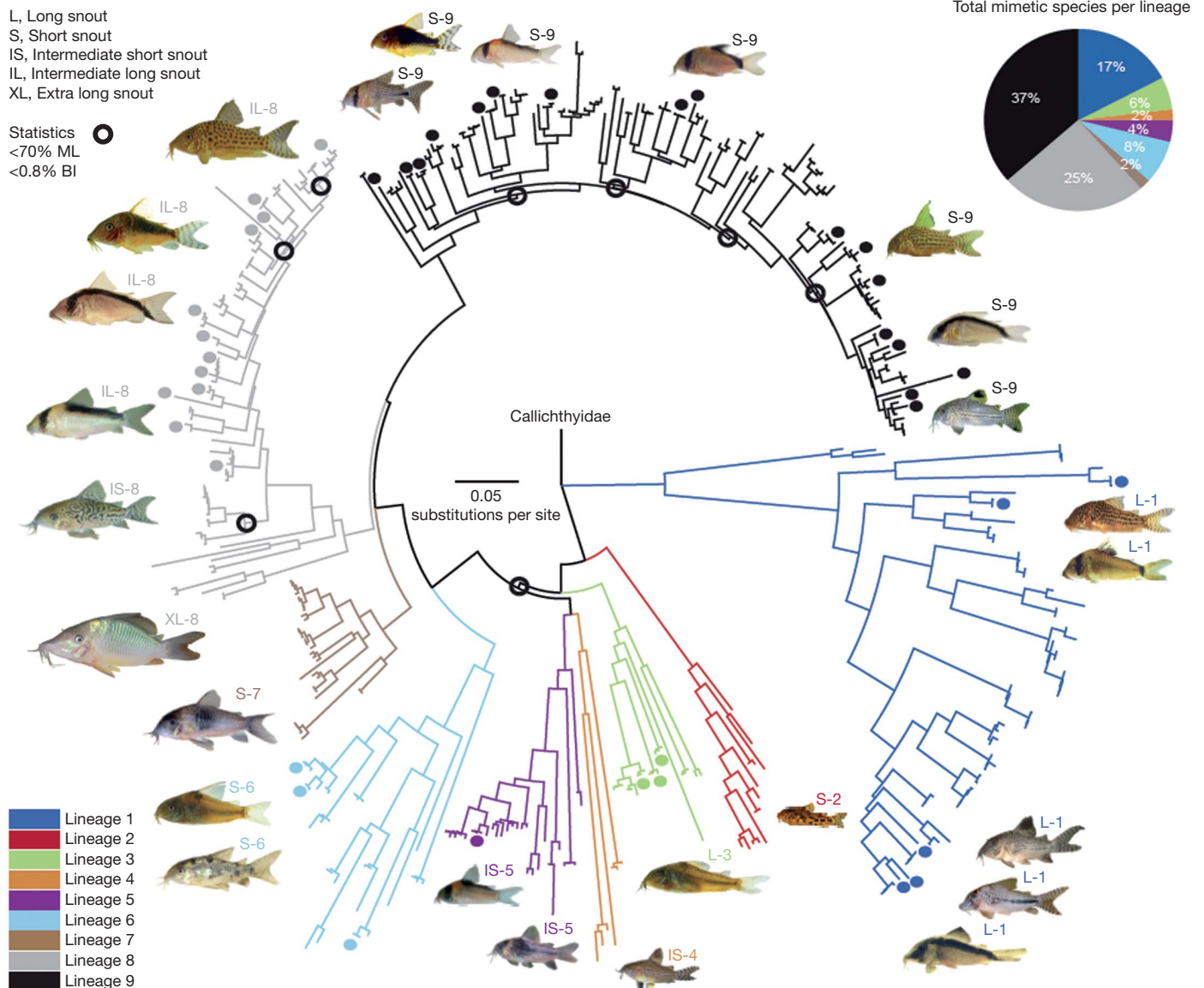


**Figure 1 | Phylogenetic relationships of Corydoradinae including co-mimics.** The pie chart shows percentage of mimetic species per lineage. Branches with mimetic species at tips are indicated with coloured circles (coded by lineage). Nodes with support below 0.8 (Bayesian inference; BI) probability and 70% (maximum likelihood; ML) are denoted with black open circles. Codes on pictures indicate snout types as determined by morphometrics and genetic lineage (L, long; S, short; IS, intermediate short; XL, extra long; IL, intermediate long). Representative images of morphotypes and colour patterns clockwise

from lineage 1: (L-1) *Corydoras maculifer*, (L-1) *C. simulatus*, (L-1) *C. sp. C109*, (L-1) *C. sp. C92*, (L-1) *C. narcissus*; (S-2) *A. poecilius*\*; (L-3) *S. prionotus*; (IS-4) *C. mamore*; (IS-5) *C. sp. CW19*, (IS-5) *C. nijsseni*; (S-6) *C. paleatus*, (S-6) *C. nattereri*; (S-7) *C. sp. CW26*; (XL-8) *C. multiradiatus*\*; (IS-8) *C. sodalis*\*; (IL-8) *C. imitator*, (IL-8) *C. sp. CW6*, (IL-8) *C. seussi*, (IL-8) *C. sp. C122*; (S-9) *C. sp. C91*, (S-9) *C. gossei*, (S-9) *C. adolfoi*, (S-9) *C. metae*, (S-9) *C. araguaiaensis*, (S-9) *C. arcuatus*, (S-9) *C. julii*. \*Non-mimetic taxa.

conspicuous but should be distinctive<sup>20</sup>, while cryptic and aposematic elements present in individual prey are not necessarily mutually exclusive<sup>21–23</sup>.

Of the 52 mimetic species, most belong to lineages 1, 8 and 9 (Fig. 1), suggesting a non-random frequency of co-occurrence between members of different lineages. In all cases, genetic distance is great enough between co-mimics for them to be considered reproductively isolated (mean pairwise mitochondrial distance =  $11.16\% \pm 4.4$  (standard deviation)). Furthermore, cytogenetic data indicate that respective members of different lineages have undergone extensive genomic duplications, with chromosome complements ranging from  $2n = 44–134$  and genome sizes ranging from 1.1–8.75 pg<sup>24,25</sup>. Most of this variation occurs between lineages; however, there is also significant variation within lineages and often between sibling species.

Trophic interactions were elucidated using stable isotopes of carbon ( $^{13}\text{C}/^{12}\text{C}$  ratio, reported as  $\delta^{13}\text{C}$ ) and nitrogen ( $^{15}\text{N}/^{14}\text{N}$  ratio, reported as  $\delta^{15}\text{N}$ ), allowing us to assess the extent of dietary overlap among co-mimics. Nitrogen isotopes are particularly informative, as values increase in a stepwise manner between trophic levels; for example, carnivore tissues have higher  $\delta^{15}\text{N}$  values than herbivore tissues<sup>26</sup>. Carbon isotope ratios ( $\delta^{13}\text{C}$ ) may change slightly with trophic level, but the major source of variation has been attributed to differences in the sources of primary production, and  $\delta^{13}\text{C}$  values are typically more useful in deriving foraging locations<sup>27,28</sup>. Significant differences ( $P < 0.001$ ) after post-hoc corrections were found in mean  $\delta^{15}\text{N}$  values within six mimicry rings composed of species belonging to different lineages, with different morphology (Table 1 and Supplementary Table 2). Niche overlap (no significant differences in mean  $\delta^{15}\text{N}$ )

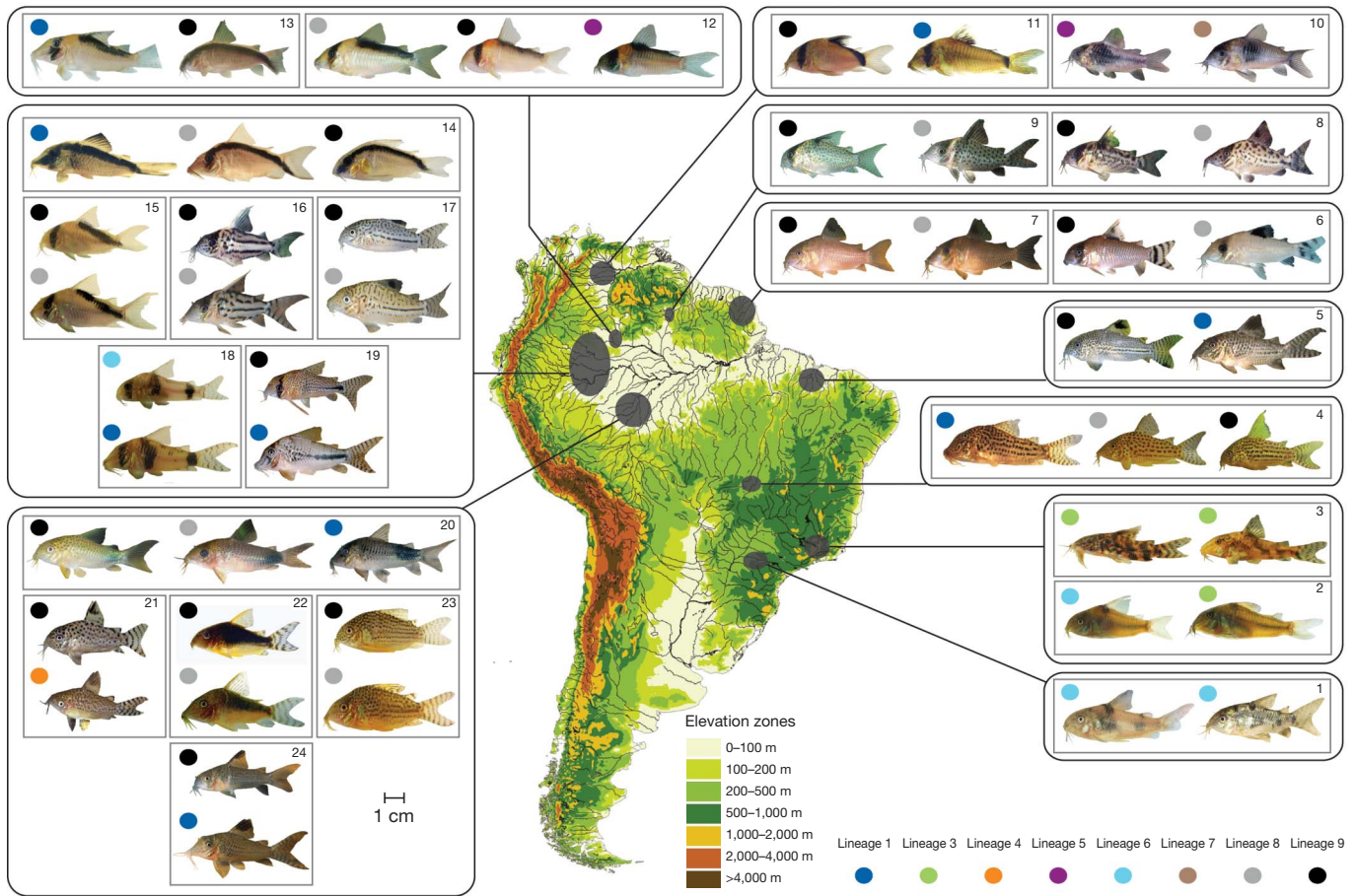


**Figure 2 | Geographical distribution of mimetic communities.** Genetic lineages are denoted by coloured circles; small grey rectangles represent independent mimetic communities numbered 1–24. Larger black rectangles indicate communities belonging to the same drainage or basin. Grey ellipses indicate approximate geographical distribution. Species images: (1) *C. paleatus*, *C. ehrhardti*; (2) *C. nattereri*, *Scleromystax prionotus*; (3) *S. barbatus*, *S. macropterus*; (4) *C. maculifer*, *C. sp. C122*, *C. araguaiaensis*; (5) *C. julii*, *C. sp. C109*; (6) *C. oiapoquensis*, *C. condisciplus*; (7) *C. sp. C135*, *C. sp. C136*; (8) *C.*

*evelynae*, *C. sp. CW13*; (9) *C. kanei*, *C. crimmeni*; (10) *C. sp. CW19*, *C. sp. CW26*; (11) *C. metae*, *C. simulatus*; (12) *C. imitator*, *C. adolfoi*, *C. nijsseni*; (13) *C. serratus*, *C. cf. arcuatus*; (14) *C. narcissus*, *C. sp. CW6*, *C. arcuatus*; (15) *C. sp. C84*, *C. sp. C156*; (16) *C. sp. CW28*, *C. pulcher*; (17) *C. trilineatus*, *C. leopardus*; (18) *C. tukano*, *C. sp. CW11*; (19) *C. sp. C91*, *C. sp. C92*; (20) *C. similis*, *C. sp. C66*, *C. ourastigma*; (21) *C. cruziensi*, *C. mamore*; (22) *C. gossei*, *C. seussi*; (23) *C. sterbai*, *C. haraldshultzi*; (24) *C. sp. C76*, *C. sp. C77*.

was only observed between two co-mimic pairs (Supplementary Fig. 5). Differences in  $\delta^{13}\text{C}$  values were significant between species in five out of the eight mimicry rings examined (Table 1 and Supplementary Table 2). Divergence of isotopic signatures reflects dietary segregation between long-snouted species compared to short-snouted species. There is a clear relationship between morphology and niche occupation in the Corydoradinae, as larger long-snouted species always occupy a lower relative ‘trophic level’ (consistently lower  $\delta^{15}\text{N}$ ) than smaller

short-snouted species (Supplementary Table 2). Minor variation in isotopic signatures could also result from physiological differences between species. However, this is unlikely here given the scale of observed differences and the close genetic affinity of Corydoradinae.

Quantifying traits with adaptive value is valuable in the study of trophic differentiation. Body size and snout or jaw morphology are particularly important traits for food acquisition in fishes<sup>29,30</sup>. We used a landmark-based geometric morphometric approach, grouping our

**Table 1 | Isotope statistics**

Site	Species comparisons	$\delta^{13}\text{C}$ (P value)	$\delta^{15}\text{N}$ (P value)	$\delta^{13}\text{C}$ (d.f., F, P)	$\delta^{15}\text{N}$ (d.f., F, P)	Test type
4	<i>C. araguaiaensis</i> versus <i>C. maculifer</i>	0.606	0.00002	42, 0.679, 0.513	42, 52.588, 0.00000	One-way ANOVA plus Tukey–Kramer
4	<i>C. araguaiaensis</i> versus <i>C. sp. C122</i>	0.957	0.00126			
4	<i>C. maculifer</i> versus <i>C. sp. C122</i>	0.569	0.00029			
12	<i>C. adolfoi</i> versus <i>C. imitator</i>	0.00002	0.00002	41, 41.02, 0.00000	41, 46.104, 0.00000	One-way ANOVA plus Tukey–Kramer
12	<i>C. adolfoi</i> versus <i>C. nijsseni</i>	0.00002	0.00004			
12	<i>C. imitator</i> versus <i>C. nijsseni</i>	0.762	0.295			
13	<i>C. arcuatus</i> versus <i>C. serratus</i>	0.00000	0.00000	39, 47.062, 0.00000	39, 128.05, 0.00000	t-test plus Bonferroni
18	<i>C. tukano</i> versus <i>C. sp. CW11</i>	0.00000	0.00000	40, 27.878, 0.00000	40, 56.858, 0.00000	t-test plus Bonferroni
2	<i>C. nattereri</i> versus <i>S. prionotus</i>	0.00522	0.00000	35, 8.914, 0.00522	35, 43.837, 0.00000	t-test plus Bonferroni
3	<i>S. barbatus</i> versus <i>S. macropterus</i>	0.00000	0.186	41, 41.823, 0.00000	42, 1.808, 0.186	t-test plus Bonferroni
1	<i>C. paleatus</i> versus <i>C. ehrhardti</i>	0.275	0.842	28, 1.112, 0.275	28, 0.041, 0.842	t-test plus Bonferroni

Site 1, Rio Tibaji; site 2, Rio Fau; site 3, east coast; site 4, Rio Araguaia; site 12, Rio Negro; site 13, Rio Negro; site 18, Rio Tiquie. Statistical comparisons are shown between species pairs (P values) and mimicry rings within sites for carbon and nitrogen ratios (d.f., degrees of freedom; F, F test statistic; P, P value). Standard Bonferroni corrected critical P = 0.025.

results in principal component analysis (PCA) and canonical variate analysis (CVA) plots by phylogenetic lineage to assess the extent of morphological conservatism within and between lineages and comimics (Supplementary Figs 6 and 7). In 92% of cases examined, mimicry rings were found to be composed of species with significant morphometric differences, an observation confirmed with pairwise *F* tests comparing partial Procrustes distances between respective comimic lineages ( $P < 0.01$  for all pairwise comparisons) (Supplementary Table 4). Key characters determining these differences include snout length, eye position and body depth, and these are probably important phenotypic traits facilitating niche differentiation, as they are directly associated with observed differences in niche occupation. Only two mimicry rings consist of species that are members of overlapping morphometric groups. Furthermore, observed morphological differences in snout and body size are phylogenetically conserved, indicative of a role for niche conservatism within lineages. Evidence from stable isotopes for eight mimicry rings and morphological analysis of all known communities suggests that ecologically relevant morphological divergence has resulted in snout-specific species assortment within mimetic communities more often than expected at random. Moreover, the majority of observed mimicry rings consist of species that have diverged in terms of resource acquisition, but converged in spatial occupation and colour pattern.

To investigate further the evolution of colour patterns among comimics we quantified the geographical distribution of colour patterns and compared them within and between communities. Mimetic *Corydoradinae* catfishes display a variety of contrasting colour pattern characteristics such as blocks of colour, bright spines, patches, bands, stripes, spots and reticulations. Using 20 different sections of the fish we scored the presence (1), absence (0), or variability (0.5) of different colour pattern characteristics (Methods). This allowed a quantification of pattern for each mimetic species that could then be compared to all other respective mimics using Euclidean pairwise distance matrices (Supplementary Fig. 8). A Mantel test revealed that sympatric comimics are more similar in colouration than those in allopatry ( $r = -0.585$ ,  $P = 0.001$ ), indicating a highly significant relationship between colour pattern and geographical distribution.

We report a diverse assemblage of vertebrate Müllerian mimics that inhabit aquatic environments through which they signal to predators foraging in two different optical modalities: water and air. We demonstrate that dietary resource partitioning coupled with morphological and phylogenetic differences determine community assembly despite the positive benefits of Müllerian mimicry. These results suggest that the benefits accrued by Müllerian co-mimics are not sufficient to overcome the need for ecological differentiation for stable long-term coexistence, thereby reinforcing the position that antagonistic interactions set ecological limits on the diversification of mutualistic communities. Despite these limits, Müllerian mimicry may increase diversification rates among allopatric communities if predation-driven directional selection simultaneously leads to convergence of colouration among sympatric taxa, but divergence among allopatric taxa. Many neotropical habitats are critically threatened by anthropogenic pollution, deforestation and river obstruction and modification. As a result we may lose many of these unique species and communities before we fully appreciate their extraordinary diversity.

## METHODS SUMMARY

A total of 425 taxa (226 operational taxonomic units) were collected or obtained from wild populations. Partial mitochondrial and nuclear DNA sequences were amplified, sequenced and aligned to construct a comprehensive molecular phylogeny for the *Corydoradinae*. Maximum likelihood and Bayesian analysis were performed on separate and concatenated data sets to test for phylogenetic relatedness of mimetic species. A total of 18 species belonging to eight different independent communities were collected to examine trophic interactions within mimicry rings using stable isotopes of carbon and nitrogen. Individual tissue samples were processed and analysed using continuous-flow isotope ratio mass spectrometry. Mimetic and non-mimetic species were photographed and

analysed using a geometric morphometric approach based on 24 homologous landmarks to identify ecologically relevant differences in shape. Multivariate plots of transformed morphometric distances were used to assess the extent of overlap in overall shape within and between different lineages of mimetic species. Colour patterns of mimetic species were quantified by dividing the lateral section of each fish into 20 subsections, which were then scored for the presence, absence, or variability of particular patterns. Using these data a matrix was created describing colour pattern based on 100 colour characters for 52 mimetic species, while a second matrix was created scoring species in terms of geographical distance (sympatric or allopatric). The two matrices were compared using a Mantel test to examine the relationship between colour patterns and geographical distance.

**Full Methods** and any associated references are available in the online version of the paper at [www.nature.com/nature](http://www.nature.com/nature).

**Received 29 April; accepted 10 November 2010.**

- May, R. M. The role of theory in ecology. *Am. Zool.* **21**, 903–910 (1981).
- Gross, K. Positive interactions among competitors can produce species-rich communities. *Ecol. Lett.* **11**, 929–936 (2008).
- Rowland, H. M., Ihalainen, E., Lindström, L., Mappes, J. & Speed, M. P. Co-mimics have a mutualistic relationship despite unequal defences. *Nature* **448**, 64–67 (2007).
- Elias, M., Gompert, Z., Jiggins, C. & Willmott, K. Mutualistic interactions drive ecological niche convergence in a diverse butterfly community. *PLoS Biol.* **6** (2008).
- Brooker, R. W. *et al.* Facilitation in plant communities: the past, the present, and the future. *J. Ecol.* **96**, 18–34 (2008).
- Callaway, R. M. Positive interactions among plants. *Bot. Rev.* **61**, 306–349 (1995).
- Stachowicz, J. J. Mutualism, facilitation, and the structure of ecological communities. *Bioscience* **51**, 235–246 (2001).
- Ruxton, G. D., Sherratt, T. N. & Speed, M. P. *Avoiding Attack* (Oxford Univ. Press, 2004).
- Fuller, I. A. & Evers, H.-G. *Identifying Corydoradinae Catfish* (Ian Fuller Enterprises, 2005).
- Nelson, J. *Fishes of the World* (John Wiley & Sons, 2006).
- Nijssen, H. Revision of the Surinam catfishes of the genus *Corydoras* (Pisces; Siluriformes; Callichthyidae). *Beaufortia* **18**, 1–75 (1970).
- Sands, D. D. *The Behaviour and Evolutionary Ecology of Corydoras adolfoi and Corydoras imitator: Studies on Two Species of Sympatric Catfish from the Upper Rio Negro, Brazil*. PhD thesis, Univ. Liverpool (1994).
- Axenrot, T. E. & Kullander, S. O. *Corydoras diphyes* (Siluriformes: Callichthyidae) and *Otocinclus mimulus* (Siluriformes: Loricariidae), two new species of catfishes from Paraguay, a case of mimetic association. *Ichthyol. Explor. Freshwat.* **14**, 249–272 (2003).
- Luz-Agostinho, K. D. G., Agostinho, A. A., Gomes, L. C. & Julio, H. F. Influence of food pulses on diet composition and trophic relationships among piscivorous fish in the upper Parana River floodplain. *Hydrobiologia* **607**, 187–198 (2008).
- Power, M. E. Depth distributions of armored catfish—Predator-induced resource avoidance. *Ecology* **65**, 523–528 (1984).
- Greven, H., Flasbeck, T. & Passia, D. Axillary glands in the armored catfish *Corydoras aeneus* (Callichthyidae, Siluriformes). *Verh. Ges. Ichthyol.* **6**, 65–69 (2006).
- Kiehl, E., Rieger, C. & Greven, H. Axillary gland secretions contribute to the stress-induced discharge of a bactericidal substance in *Corydoras sterbai* (Callichthyidae, Siluriformes). *Verh. Ges. Ichthyol.* **6**, 111–115 (2006).
- Wright, J. J. Diversity, phylogenetic distribution, and origins of venomous catfishes. *BMC Evol. Biol.* **9**, 282 (2009).
- Müller, F. Über die vorteile der mimicry bei schmetterlingen. *Zool. Anz.* **1**, 54–55 (1878).
- Endler, J. A. & Mappes, J. Predator mixes and the conspicuousness of aposematic signals. *Am. Nat.* **163**, 532–547 (2004).
- Merilaita, S. & Ruxton, G. D. Aposematic signals and the relationship between conspicuousness and distinctiveness. *J. Theor. Biol.* **245**, 268–277 (2007).
- Wüster, W. *et al.* Do aposematism and Batesian mimicry require bright colours? A test, using European viper markings. *Proc. R. Soc. Lond. B* **271**, 2495–2499 (2004).
- Wright, J. J. Conservative coevolution of Müllerian mimicry in a group of rift lake catfish. *Evolution* doi:10.1111/j.1558-5646.2010.01149.x (22 October 2010).
- Hinegardner, R. & Rosen, D. E. Cellular DNA content and evolution of Teleostean fishes. *Am. Nat.* **106**, 621–644 (1972).
- Oliveira, C., Almeida-Toledo, L. F., Mori, L. & Toledo-Filho, S. A. Extensive chromosomal rearrangements and nuclear-DNA content changes in the evolution of the armored catfishes genus *Corydoras* (Pisces, Siluriformes, Callichthyidae). *J. Fish Biol.* **40**, 419–431 (1992).
- Peterson, B. J. & Fry, B. Stable isotopes in ecosystem studies. *Annu. Rev. Ecol. Syst.* **18**, 293–320 (1987).
- Rubenstein, D. R. & Hobson, K. A. From birds to butterflies: animal movement patterns and stable isotopes. *Trends Ecol. Evol.* **19**, 256–263 (2004).
- West, J. B., Bowen, G. J., Cerling, T. E. & Ehleringer, J. R. Stable isotopes as one of nature's ecological recorders. *Trends Ecol. Evol.* **21**, 408–414 (2006).

29. Clabaut, C., Bunje, P. M. E., Salzburger, W. & Meyer, A. Geometric morphometric analyses provide evidence for the adaptive character of the Tanganyikan cichlid fish radiations. *Evolution* **61**, 560–578 (2007).
30. Genner, M. J., Turner, G. F., Barker, S. & Hawkins, S. J. Niche segregation among Lake Malawi cichlid fishes? Evidence from stable isotope signatures. *Ecol. Lett.* **2**, 185–190 (1999).

**Supplementary Information** is linked to the online version of the paper at [www.nature.com/nature](http://www.nature.com/nature).

**Acknowledgements** This research was funded by NERC small grant (NE/C001168/1), NERC Mass Spectrometry access grant (NE/F007205/1) awarded to M.I.T., and a NERC PhD studentship (NE/F007205/1) awarded to M.A.A. Research was also supported by UNESP, Brazil. We would like to thank the staff and students of UNESP, Botucatu, Brazil for facilities and research support during fieldwork including P. Venere for helping to collect samples in the Rio Araguaia, and M. Britto for identifying samples. We would also like to thank B. Emerson and G. Ruxton for their suggestions and critical evaluation of the manuscript. We thank J. Montoya-Burgos, M. Sabaj Perez, I. Fuller,

H.-G. Evers, M. Walters and K. Mathiesen for providing tissue samples and photographs, and A. Orchard for photographing preserved specimens.

**Author Contributions** M.I.T. conceived the study, contributed to all data collection, analysis and writing and supervised M.A.A.; M.A.A. conducted fieldwork, DNA sequencing, stable isotope analysis, morphology and colour pattern analysis, data analysis and writing. C.O. co-supervised M.A.A. and organized and participated in field sampling and writing. M.M. and R.A.R.M. conducted DNA sequencing and stable isotope analysis, respectively; J.N. provided stable isotope advice and guidance; and S.C. co-supervised M.A.A. and contributed to writing.

**Author Information** Sequence data have been deposited in GenBank (<http://www.ncbi.nlm.nih.gov/genbank/>) with accession numbers detailed in Supplementary Table 1. Reprints and permissions information is available at [www.nature.com/reprints](http://www.nature.com/reprints). The authors declare no competing financial interests. Readers are welcome to comment on the online version of this article at [www.nature.com/nature](http://www.nature.com/nature). Correspondence and requests for materials should be addressed to M.I.T. ([m.taylor@bangor.ac.uk](mailto:m.taylor@bangor.ac.uk)).

## METHODS

**Sample acquisition and phylogenetic analysis.** A total of 425 taxa (226 operational taxonomic units with multiple representatives when available) were obtained from wild populations collected by the authors, or purchased as wild-caught aquarium imports (Supplementary Table 1). Species for which we lack genetic material (*C. mamore*, *C. evelynae*, *C. ourastigma*, *C. crimmeni*, *C. sp. CW19*, *C. sp. CW26*, *C. sp. C135*, *C. sp. C76*, *C. sp. C77*) were identified and assigned to lineages on the basis of geometrical morphometric analysis, with which it is possible to differentiate between lineages. Partial sequences of 12S rRNA, 16S rRNA, ND4, tRNA<sup>His</sup>, tRNA<sup>Ser</sup>, cytochrome *b* (Cytb) and recombination activating gene (RAG1) were amplified for 425 taxa, and a nuclear intron from F-reticulon-4 amplified for 24 taxa, using the polymerase chain reaction (PCR) with the primers detailed in Supplementary Table 4. All products were sequenced in both directions using Big Dye terminator technology (Applied Biosystems). The quality of chromatograms was visually inspected and contigs were assembled using Geneious v 4.7 (ref. 31). A total of 50 alternative alignments for the 12s, 16s and F-reticulon-4 markers were generated using ProAlign<sup>32</sup>, discarding unstable positions that differed more than 50% (gap opening penalty 7–15; gap extension penalty 3–7). The ND4, Cytb and RAG1 genes were aligned with MUSCLE<sup>33</sup>, and all alignments were checked by eye. Substitution saturation and base compositional biases were tested for each gene and partition. Model selection was performed using the hLRT criterion under a fixed BIONJ-JC topology in JModelTest<sup>34</sup>. All data were partitioned by gene and coding position where appropriate. Incongruent length difference tests were performed to test for heterogeneity between nuclear and mitochondrial data sets. Subsequent analyses were performed on the following data sets: (1) MIT: all mitochondrial markers (for practical purposes, 12s + 16s considered as a single partition, as were tRNA<sup>His</sup> + tRNA<sup>Ser</sup>); (2) MITNUC: the MIT and RAG1 data combined; (3) MITNUC2: a smaller subset of the MITNUC data combined with the F-reticulon-4 intron for 25 representative taxa; (4) RAG1: a single nuclear marker independent of mitochondrial data. We rely primarily on the MIT data set as it represents the largest sample of linked markers, and use the others for comparisons. RAxML<sup>35</sup> using the web server RAxML BlackBox<sup>36</sup> was used for maximum likelihood analyses under a mixed partition model for all analyses. Random starting trees were used for each independent maximum likelihood (ML) tree search and all other parameters were set on default. Topological robustness was investigated using 500 non-parametric bootstrap replicates. Analyses were conducted under both GTR+G and GTR+I+G to assess whether implementing P-Invar and Gamma together affected parameter estimation. Bayesian analyses were performed using MrBayes v3.1.2 (ref. 37) Metropolis-coupled Markov chain Monte Carlo (MCMC) runs were set with random starting trees, one cold and three heated chains for 30 million generations, sampled every 1,000 generations for all data sets. We used the default uniform Dirichlet distribution for the base frequencies, and default prior distributions for all other parameters. Bayesian posterior probabilities were then calculated from the sample points after MCMC convergence. To ensure that analyses were not trapped in local optima, two independent MCMC runs were performed. Topologies and posterior clade probabilities from different runs were compared for congruence using Tracer 1.4 (ref. 38), to ensure adequate estimated sample sizes and ensure adequate mixing of parameters. All trees estimated before convergence were discarded. Trees from different runs were then combined using LogCombiner<sup>39</sup>, and maximum clade credibility trees (mean node heights) were estimated using TreeAnnotator<sup>39</sup>.

**Geometric morphometrics.** A total of 200 preserved individuals, representing over 120 different species (including all mimetic taxa), were photographed and used for digital landmark-based morphometric analysis of body shape (Supplementary Table 1; asterisks denote species analysed using morphometrics). We defined 24 easily identifiable homologous landmarks (see Supplementary Fig. 9), including two for scaling (ruler 1 cm). Photographs with landmarks were digitalized (using tpsDig by F. J. Rohlf, available at <http://life.bio.sunysb.edu/morph/>), and converted to coordinates under Procrustes superimposition (using CoordGen6 by H. D. Sheets, part of the Integrated Morphometrics Package (IMP) at <http://www2.canisius.edu/~sheets/morphsoft.html>) to describe shape change independent of size (removing potential ontogenetic effects and issues of allometry). We used PCAGEN and CVAGEN packages from IMP to create multivariate plots of Procrustes superimpositions (with axes normalized to lengths of one for all plots and outputs) and vectors of CV coefficients (scaled to a length of one) respectively. We also conducted pairwise comparisons of co-existing lineages to check for statistically significant differences in shape using Goodall's *F*-tests as implemented

in TwoGroup6 (Supplementary Table 3). Deformation plots were generated to identify landmarks contributing to shape changes across lineages and between co-mimics.

**Stable isotope analysis.** Muscle tissue was collected from 20 individuals (where possible) from 18 species belonging to eight different independent mimicry rings. All samples were dried overnight in an incubator at 60 °C to constant weight before storage in 1.5-ml centrifuge tubes containing silica gel. On return to the laboratory, the tissue samples were homogenized to a fine powder using a mortar and pestle. Approximately 0.7 mg of homogenized muscle was weighed out and distributed into tin capsules for analysis by continuous-flow isotope ratio mass spectrometry, using a Costech (model ECS 4010) elemental analyser with a ThermoFinnigan Delta Plus XP mass spectrometer. We used a number of gelatine and alanine standards (two for every ten samples) to obtain a standard deviation of 0.2‰ for δ<sup>15</sup>N and 0.1‰ for δ<sup>13</sup>C. Samples of ground tryptophan were incorporated into each run as independent isotope standards and to calculate C and N abundance. These internal laboratory standards have been measured against secondary international isotope standards provided by the NIST and IAEA. All data are referenced to the primary international standards atmospheric nitrogen (AIR δ<sup>15</sup>N) and Vienna-PeeDee Belemnite (V-PDB δ<sup>13</sup>C). The effects of lipid extraction were checked on a subset of samples using a 10:5:4 methanol/chloroform/water extraction, repeated three times to obtain a clear supernatant<sup>40</sup>. Isotope values from lipid and non-lipid extracted samples of the same aliquot were the same. Separate aliquots of muscle tissue were used to obtain carbon and nitrogen isotope analyses. All resulting carbon and nitrogen stable isotope ratios were checked for conformity to a normal distribution and analysed with one-way ANOVAs for mimicry rings consisting of >2 species, followed by Tukey–Kramer post-hoc tests. In cases with only two species, we used a two-sample *t*-test to compare means, followed by Bonferroni post-hoc corrections. Significant differences in stable isotope ratios were then used to determine the degree of dietary differentiation to identify communities composed of species that partition trophic resources from those that do not. However, stomach contents analyses were not conducted and therefore these results cannot be extended to quantify dietary overlap (that is, the proportion of food items shared between coexisting species).

**Colour pattern analysis.** Pictures of live fishes were obtained from specimens caught in the wild and later kept under standardized aquarium conditions. Colour patterns (not hue) of mimetic species were quantified by dividing the lateral section of each fish into 20 subsections (Supplementary Fig. 9). Subsections were then scored for the presence (1), absence (0), or variability (0.5) of particular patterns (contrasting bands, reticulations, spots, blotches, bright patches, dark patches, stripes, uniform brown and lack of patterns). Using these data we created a matrix describing colour pattern based on 100 characters for 52 mimetic species, and generated a pairwise Euclidian distance matrix using MVSP 3.1 (ref. 41). A second pairwise matrix was created to score the respective members of independent mimicry rings in terms of geographical distribution, where sympatric species were scored 1, whereas allopatric species were scored 0. The significance of the relationship between the two matrices was investigated using a Mantel test with 10,000 permutations using the software zt<sup>42</sup>.

31. Drummond, A. J. *et al.* Geneious v4.7 (<http://www.geneious.com>) (2009).
32. Loytynoja, A. & Milinkovitch, M. C. SOAP, cleaning multiple alignments from unstable blocks. *Bioinformatics* **17**, 573–574 (2001).
33. Edgar, R. C. MUSCLE: a multiple sequence alignment method with reduced time and space complexity. *BMC Bioinf.* **5**, 1–19 (2004).
34. Posada, D. jModelTest: Phylogenetic model averaging. *Mol. Biol. Evol.* **25**, 1253–1256 (2008).
35. Stamatakis, A. RAxML-VI-HPC: Maximum likelihood-based phylogenetic analyses with thousands of taxa and mixed models. *Bioinformatics* **22**, 2688–2690 (2006).
36. Stamatakis, A., Hoover, P. & Rougemont, J. A rapid bootstrap algorithm for the RAxML web servers. *Syst. Biol.* **57**, 758–771 (2008).
37. Huelsenbeck, J. P. & Ronquist, F. MRBAYES: Bayesian inference of phylogenetic trees. *Bioinformatics* **17**, 754–755 (2001).
38. Rambaut, A. & Drummond, A. J. Tracer v1.4 (<http://beast.bio.ed.ac.uk/Tracer>) (2004).
39. Drummond, A. J. & Rambaut, A. BEAST: Bayesian evolutionary analysis by sampling trees. *BMC Evol. Biol.* **7** (2007).
40. Pinnegar, J. K. & Polunin, N. V. C. Differential fractionation of δ<sup>13</sup>C and δ<sup>15</sup>N among fish tissues: implications for the study of trophic interactions. *Funct. Ecol.* **13**, 225–231 (1999).
41. Kovach, W. L. MVSP—A MultiVariate Statistical Package for Windows, version 3.1 (Kovach Computing Services, 1999).
42. Bonnet, E. & Van de Peer, Y. zt: a software tool for simple and partial Mantel tests. *J. Stat. Softw.* **7**, 1–12 (2002).